Electro-Conducting Properties of Charge-Transfer Salts Based on Cationic and Anionic Platinum Dithiolenes − Crystal Structure of $[Pt(Me_2pipdt)_2][Pt(dtcr)_2]$

Paola Deplano,*[a] Maria Laura Mercuri,[a] Luciano Marchiò,[b] Luca Pilia,[a] Marco Salidu,[a] Angela Serpe,[a] Francesco Congiu,[c] and Samuele Sanna[c]

Dedicated to Prof. Emanuele F. Trogu on the occasion of his recent retirement

Keywords: Sulfur ligands / Platinum / Charge-transfer / Conducting materials

The structure/property relationship of the following CT salts, $[M(R_2pipdt)_2][M(mnt)_2]$ (where R_2pipdt = *N*,*N*′-dialkylpiperazine-2,3-dithione; mnt = maleonitrile-2,3-dithiolate), [R = Me, M = Pd (**1a**) and Pt (**2a**); R = Et, M = Pt (**2b**)],which were previously characterised, and $[Pt(R_2pipdt)_2][Pt(dtcr)_2]$ [R = Me, (**3a**); R = Et, (**3b**); dtcr = 4,5-disulfanylcyclopent-4-ene-1,2,3-trionate, known as dithiocroconate] are investigated here. These salts show strong near IR CT bands and semiconducting behaviour. The structural features of **3a** are similar to those found for **2a**: approximately square planar $[Pt(Me_2pipdt)_2]$ dications and regular square planar $[Pt(dtcr)_2]$ dianions form an infinite anion–cation one-dimensional stack along the *c* axis with a Pt···Pt *c*/2 distance of 3.408 (1) Å. In **3a**, a net of weak interactions between the N and O atoms of the cation and of the anion contributes to the alignment of **3a** in the stack. However, these interactions do not overcome the less favourable redox properties of the components, that is, promoting CT interactions with respect to the corresponding mnt salts. The specific electrical conductivity of pressed powder pellets ranges from 10^{-11} to $10^{-5}\ \Omega^{-1}cm^{-1}$ at room temperature, follows the Arrhenius law with activation energies in the range of 0.2–0.6 eV, and is related to the driving force of the electron transfer. Preliminary photoconductivity measurements performed on the two relatively more conducting samples, **2a** and **2b**, show a gain in current during illumination, similarly to that observed in organic–inorganic photoconductor CT salts $C[ML_2]$ (C^{2+} is 2,2′ or 4,4′-bipyridinium or similar derivatives, L^{2-} = dithiolato), which have been extensively investigated by the Kisch group. Crystal data for **3a**: triclinic, $P\bar{1}$; $Z = 2$; $T = 293(2)$ K; $a = 8.683(2)$ Å, $b = 14.009(5)$ Å, $c = 6.815(2)$ Å; $\alpha = 100.58(4)°$, $\beta = 98.99(3)°$, $\gamma = 100.69(3)°$. *R* indices (all data) $R1 = 0.0516$, $wR2 = 0.1412$.

Introduction

Among several applications in the molecular material field,[1] anionic, square planar d^8 metal bis-dithiolene complexes have been used to prepare ion-pair CT photoconducting salts of the type $\{(C^{2+})[ML_2]^{2-}\}$, (M = Ni, Pd, Pt; L^{2-} = dithiolato) where C^{2+} is a redox-active organic donor such as 4,4′ and 2,2′ bipyridinium derivatives.[2] An extensive investigation on these organic–inorganic CT salts by Kisch's group has led to an understanding of the main factors that affect the structure/property relationship. The supramolecular interaction between the ionic components is reflected by the presence of a strong CT band in the diffuse reflectance spectra of these salts, which exhibit electrical semiconducting behaviour. By applying the "Marcus-Hush model",[3] a linear correlation between thermal and optical electron transition and a linear correlation between the specific electrical conductivity and the free activation energy for the electron transfer is observed. Moreover these CT salts show interesting photoconducting properties. It has been shown that the planarity of the components and their capability to undergo minor structural changes on electron transfer are crucial factors for improving the CT interaction. Thus a rational synthesis of the desired products would allow us to tune the conductivity by a proper selection of the component ions. This prompted us to use metal dithiolenes as the two components of CT salts, extending the investigation from the largely investigated fully organic and organic–inorganic systems to the less common fully inorganic ones.[4] In fact, in d^8 metal dithiolenes the planarity of the central core is maintained by the metal atom which imposes the square planar geometry, while the electronic properties depend on the distribution of the π electrons in the $(C_2S_2)_2M$ core (14 electrons of which four

[a] Dipartimento di Chimica Inorganica ed Analitica, Università di Cagliari,
Cittadella di Monserrato, 09042 Monserrato, Cagliari, Italy
Fax: +39-070-675-4456
E-mail: deplano@unica.it
[b] Dipartimento di Chimica Generale ed Inorganica, Chimica Analitica, Chimica Fisica, Università di Parma,
Parco Area delle Scienze 17A, 43100 Parma, Italy
[c] Dipartimento di Fisica, Università di Cagliari,
Cittadella di Monserrato, 09042 Monserrato, Cagliari, Italy

belong to the metal in the uncharged complex).[5] These species have a rich redox chemistry and the nature of their most accessible status is indicative of the basic *push* or *pull* character of the ligand. The nature of the substituents at the C_2S_2 moieties determines the stabilization of the ML_2 complex with a charge that varies between +2 and –2. The latter limits are due to the fairly isolated frontier MOs (HOMO and LUMO in the uncharged complex), which have π character and can be either empty or populated. In general, C_2S_2 π-donor substituents (*push*) in symmetric complexes raise the energy of both the HOMO and the LUMO so that the former is also preferentially depopulated (cationic complexes). In contrast, π-acceptor substituents (*pull*) lower the energies of the two levels and favour an anionic state of the complex. Thus mnt complexes (mnt = maleonitrile-2,3-dithiolate, *pull* ligand) are most readily synthesized as dianions while the R_2pipdt ones (R_2pipdt = *N*,*N*′-dialkylpiperazine-2,3-dithione, *push* ligand) are synthesized as dications.[6] On the basis of the above, new CT salts $[M(R_2pipdt)_2][M(mnt)_2]$ (M = Pd and Pt) have been recently described.[7,8] In the solid state these salts show features similar to those of $(C)[ML_2]$ compounds, where the acceptors (C) do not deviate too much from planarity.[2] In this paper the dark- and photo-conducting properties of $[M(R_2pipdt)_2][M(mnt)_2]$ {[R = Me, M = Pd (**1a**) and Pt (**2a**); R = Et, M = Pt (**2b**)]}, as well as of the novel salts of $[Pt(R_2pipdt)_2][Pt(dtcr)_2]$ (R = Me, (**3a**); R = Et, (**3b**); dtcr = 4,5-disulfanylcyclopent-4-ene-1,2,3-trionate) are reported; the structural characterization of **3a** is also described. The substitution of mnt by dtcr in **3** was performed in order to investigate the influence of the different redox potentials and of the electron-rich oxo-groups of the anionic component on the properties of these CT salts.

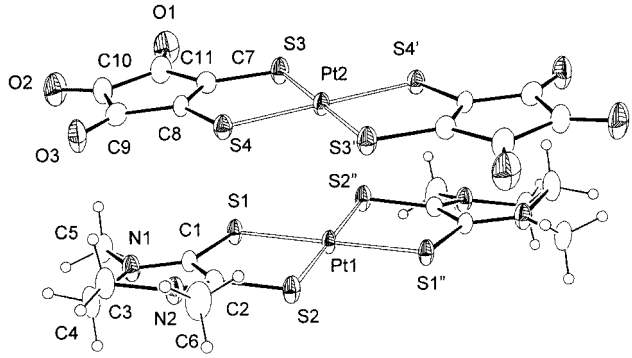

Figure 1. Ortep drawing of $[Pt(Me_2pipdt)_2][Pt(dtcr)_2]$ at the 30% probability level. (′) = –*x*, –*y*, –*z*. (″) = –*x*, –*y*, 1 – *z*.

Table 1. Selected bond lengths [Å] and angles [°] with estimated standard deviations in parentheses for $[Pt(Me_2pipdt)_2][Pt(dtcr)_2]$.

	Cation		
Pt(1)–S(1)	2.289(2)	C(1)–C(2)	1.493(9)
Pt(1)–S(2)	2.287(2)	N(1)–C(1)	1.317(9)
S(1)–C(1)	1.683(6)	N(2)–C(2)	1.311(9)
S(2)–C(2)	1.685(7)		
S(1)–Pt(1)–S(2)	88.48(6)	C(2)–N(2)–C(3)	122.1(6)
C(1)–N(1)–C(5)	123.1(6)	C(6)–N(2)–C(3)	117.1(6)
C(4)–N(1)–C(5)	115.7(7)	C(2)–N(2)–C(6)	120.2(6)
C(1)–N(1)–C(4)	121.0(6)		
	Anion		
Pt(2)–S(3)	2.312(2)	C(7)–C(8)	1.40(1)
Pt(2)–S(4)	2.309(2)	C(11)–O(1)	1.22(1)
S(3)–C(7)	1.696(8)	C(10)–O(2)	1.20(1)
S(4)–C(8)	1.705(7)	C(9)–O(3)	1.24(1)
S(4)–Pt(2)–S(3)	90.23(7)	C(7)–C(8)–C(9)	110.4(7)
C(8)–C(7)–S(3)	123.0(5)	C(9)–C(8)–S(4)	125.6(6)
C(11)–C(7)–S(3)	126.9(6)	C(7)–C(8)–S(4)	123.9(5)
C(8)–C(7)–C(11)	110.1(7)		

Results and Discussion

Preparations and Structures

$[Pt(R_2pipdt)_2][Pt(dtcr)_2]$ [where R = Me (**3a**); R = Et (**3b**)] were obtained by metathesis by treating equimolar amounts of $[Pt(R_2pipdt)_2](BF_4)_2$[7] with $(Bu_4N)_2[Pt(dtcr)_2]$[9] in CH_3CN. Crystals of **3a** suitable for X-ray characterization were grown by using a three-compartment diffusion cell, as described in the Exp. Sect.[10] A molecular drawing of the ionic complex components is depicted in Figure 1, selected bond lengths and angles are reported in Table 1.

In $[Pt(dtcr)_2]^{2-}$ and $[Pt(Me_2pipdt)_2]^{2+}$ the platinum atoms lie on inversion centres and are in a square planar geometry. They are bound by four sulfur atoms from two ligands. The complex cation and the complex anion are alternate and run parallel to the *c* crystallographic axis exhibiting a metal–metal interaction [Pt(1)–Pt(2) = 3.408(1) Å]. Despite the fact that the dtcr ligand can be formally formulated as a dithiolate, its C–S bond lengths are not significantly different from the ones observed for the dithione ligand (Me_2pipdt) in the complex cation (see Table 1). This is ascribed to a negative charge-delocalization on the oxo groups of the ligand (see Scheme 1). In fact, the C(9)–O(3) and C(11)–O(1) bonds are significantly longer than the C(10)–O(2) bond as they are in close proximity to the C(8)–S(4) and C(7)–S(3) groups, respectively, and the Pt–S bond lengths for the complex cation and the complex anion are only slightly different (Table 1). As regards the Me_2pipdt ligand, the thioamide groups are not coplanar {τ[S(1)–C(1)–C(2)–S(2)] = –16.9(8)°} and the C(1)–C(2) bond length [1.493(9) Å] is indicative of a single bond between these two atoms excluding an electron delocalisation between the thioamide moieties.

The ring conformation of the Me_2pipdt ligand {τ[N(1)–C(3)–C(4)–N(2)] = –53.0(9)°} limits the stacking between the cationic and anionic complexes; in fact they are skewed with respect to each other by ca. 45° {τ[S(1)–Pt(1)–Pt(2)–S(4)] = 43.75(7)°}.

A net of weak interactions between the N(1) and O(3) atoms [3.40(1) Å] of the cation and anion contributes to the alignment of $[Pt(Me_2pipdt)_2][Pt(dtcr)_2]$ along the *c* axis. The O(1)–N(2) intermolecular interaction [3.40(1) Å] generates a layer in the [0 1 0] crystallographic plane (Figure 2). To the best of our knowledge structural data on the [Pt-

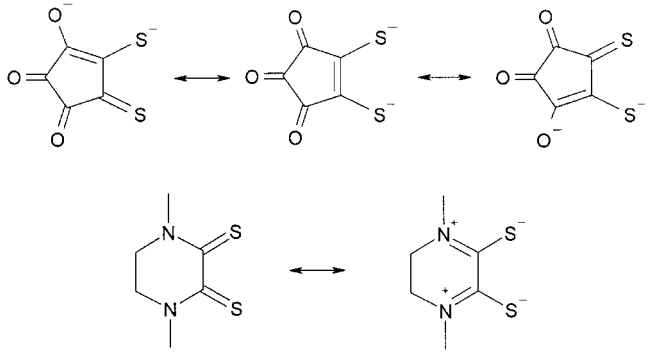

Scheme 1.

$(dtcr)_2]^{2-}$ complex appear here for the first time and are consistent with those found in the crystal structures of $[Bu_4N]_2[ML_2]\cdot I_2$ (where L = 2-dicyanomethylene-4,5-disulfanylcyclopent-4-ene-1,3-dionate; M = Pd, Pt)[9] and of $(Ph_4P)_3[Co(dtcr)_3]\cdot 0.6$ acetone.[11]

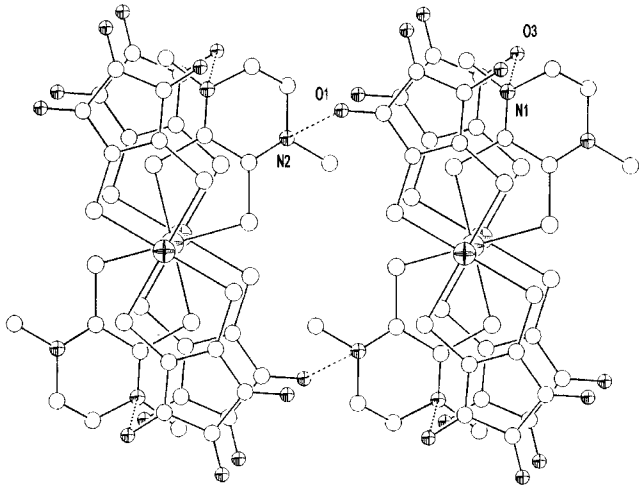

Figure 2. Perspective view of the unit cell content of $[Pt(Me_2pipdt)_2]$-$[Pt(dtcr)_2]$. Projection along the *c* axis.

Electronic Spectral Features

The comparison of the diffuse reflectance (DR) spectra of $[Pt(Me_2pipdt)_2][Pt(dtcr)_2]$ (**3a**) with those of $[Pt(Me_2pipdt)_2](BF_4)_2$ and $(Bu_4N)_2[Pt(dtcr)_2]$ is reported in Figure 3. In the spectrum of **3a**, one adjunctive, strong, long-wavelength absorption appears at 960 nm (930 nm for **3b**). Type **1** $[Pd(Me_2pipdt)_2][Pd(mnt)_2]$ and **2** $[Pt(R_2pipdt)_2]$-$[Pt(mnt)_2]$ (R = Me, Et) salts, where the redox-active planar anions and cations show a similar, alternating stacking, exhibit similarly strong near infrared peaks. These long wavelength absorptions are assigned to intermolecular charge transfer (ICT) transitions from the negatively charged to the positively charged complex.

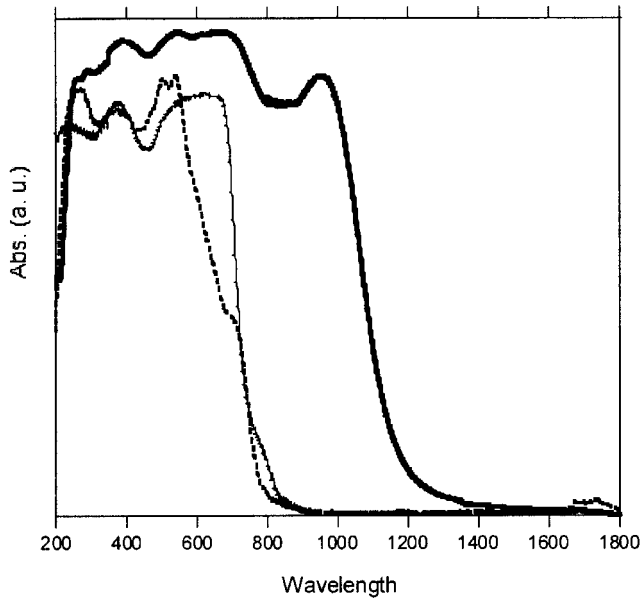

Figure 3. The diffuse reflectance spectra of $[Pt(Me_2pipdt)_2][Pt(dtcr)_2]$ (thick line) and, for comparison, of $[Pt(Me_2pipdt)_2](BF_4)_2$ (dotted line) and $(Bu_4N)_2[Pt(dtcr)_2]$ (thin line). The absorbances are reported in arbitrary units.

Theoretical calculations based on approximate Extended Hückel methods by using the CACAO program[12] have been performed to calculate the frontier orbitals of the cation and of the anions. These orbitals are π-type orbitals, and while a significant contribution of the metal d_{yz} orbital to the HOMOs occurs, the contribution of the metal to the LUMOs is negligible. The transition from the dithiolene metallate donor (HOMO) to the dicationic dithiolene acceptor (LUMO), symmetry allowed, will have charge-transfer character. The nature of the LUMO of the $[M(R_2pipdt)_2]^{2+}$ which is a π* ligand orbital can explain the observed similarity with the behaviour of $C[ML_2]$ Kisch salts (C^{2+} is almost planar, i.e. 2,2′ or 4,4′-bipyridinium derivatives, L^{2-} = dithiolato) where the CT peaks are assigned to a π→π* transition from the same platinum (or nickel) dithiolato donor to a planar organic acceptor based on bipyridinium cations (C^{2+}). The energy of the CT transition is relatable to the driving force of electron transfer from the cation to the anion ($[C]^{2+} + [A]^{2-} \rightarrow [C]^{+} + [A]^{-}$) through the following, modified Hush relation [Equation (1)].

$$E_{IPCT} = \chi + \Delta G_{12} \quad (1)$$

[E_{IPCT} is obtained from the IPCT peak in the reflectance spectra, χ represents the total reorganization energy and ΔG_{IP} is obtained from the components' redox potential difference, $E(C^{2+/+}) - E(A^{-/2-})$]. The redox features of the cation[7,13] and of the anion[9] have been previously reported. The reversible processes of interest here are shown below:

$$[Pt(R_2pipdt)_2]^{2+} \underset{1e^-}{\overset{E_{1/2}}{\rightleftharpoons}} [Pt(R_2pipdt)_2]^{+}$$

$$[Pt(dtcr)_2]^{-} \underset{1e^-}{\overset{E_{1/2}}{\rightleftharpoons}} [Pt(dtcr)_2]^{2-}$$

Moreover, the free activation enthalpy of thermal electron transfer can be calculated according to Equation (2).

$$\Delta G^* = E^2_{IPCT}/4(E_{IPCT} - \Delta G_{12}) \quad (2)$$

The E_{IPCT}, ΔG_{12}, ΔG^* values, and the reduction potentials related to $[Pt(R_2pipdt)_2][Pt(dtcr)_2]$, as well as data for $[M(R_2pipdt)_2][M(mnt)_2]$, are reported in Table 2. The more positive reduction potential of $[Pt(dtcr)_2]^{-/2-}$ with respect to the corresponding mnt derivative is in agreement with the higher charge delocalisation in the dtcr ligand. Accordingly the position of the CT transition falls at higher energies.

Infrared results are also in agreement with a CT anion–cation description for **3a** and **3b**. The ν(CN) vibration of the ligand of the $[Pt(R_2pipdt)_2]^{2+}$ dication can be used as a probe to evaluate the extent of the charge transfer from the dianion to the dication. This vibration appears as a strong peak near 1550 cm^{-1} in the tetrafluoborate. When the dication accepts charge from the donor (the dianion), a partial population of the LUMO orbital that has CN antibonding character (see Figure 4) is expected. This should produce a shift of ν(CN) to lower frequencies, as observed, although these shifts do not strictly correlate with ΔG_{12}. Differently to what observed in mnt[14] and dmit[15] complexes, where the ν(C=C) of the bond vicinal to sulfur atoms is very sensitive to the charge of the complexes (due to the main C=C bonding contribution to the HOMO in the dianion), no similar ν(C=C) vibration sensitive to the charge is observed in the $[Pt(dtcr)_2]^{2-}$ salts in Table 3. This is related to the different nature of the HOMO (see Figure 4), with no corresponding C=C bonding contribution. Instead an extensive delocalisation involving also the peripheral C=O groups exists.[16] Thus a change in the charge, distributed over the entire complex, has a slight effect on any single vibration, as observed.

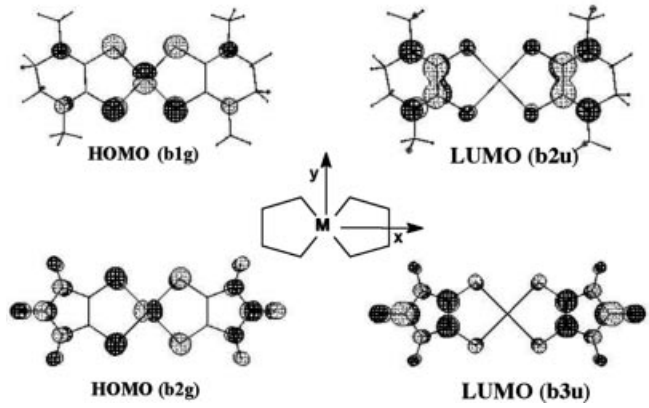

Figure 4. Frontier MOs of $[Pt(Me_2pipdt)_2]^{2+}$ and of $[Pt(dtcr)_2]^{2-}$.

Table 3. Most significant IR peaks. Spectra recorded on KBr pellets.

	ν(C=N) cm^{-1}	ν(C=O) cm^{-1}
$[Pt(R_2pipdt)_2](BF_4)_2$	1550 (R = Me) 1546 (R = Et)	
$(Bu_4N)_2[Pt(dtcr)_2]$		1683, 1668 sh, 1636
$[Pt(Me_2pipdt)_2][Pt(dtcr)_2]$	1541	1684, 1663, 1629
$[Pt(Et_2pipdt)_2][Pt(dtcr)_2]$	1529	1670, 1657, 1639

Conductivity Measurements

The above discussion shows that the structural and optical properties of this new class of ion-pair CT salts, $[M(R_2pipdt)_2][ML_2]$, are similar to those of the organic–inorganic Kisch salts, $C[ML_2]$. The electrical specific conductivity of Kisch salts gave values ranging from 10^{-10} to 10^{-3} $\Omega^{-1}cm^{-1}$ and these values are related to ΔG_{12} and ΔG^*. Moreover these salts exhibit photoconductive properties. In order to find further support in comparing the behaviour of metal-anion-dithiolene/metal-cation-dithiolene and metal-anion-dithiolene/viologen, ion pairs the dark- and photo-conductive properties of these salts were investigated.

Table 2. Reduction potentials of component ions, free reaction and activation enthalpies of the electron transfer between ions and ion-pair charge-transfer band of solid ion pairs.

$[M(R_2pipdt)_2][MA_2]$	E ($C^{2+/+}$) [V][a]	E ($A^{-/2-}$) [V][a]	E_{IPCT} [eV]	ΔG_{12} [V]	ΔG^* [eV]
M = Pt; R = Me; A = mnt (**2a**)	–0.13	+0.21	0.98	+0.34	0.37
M = Pt; R = Et; A = mnt (**2b**)	–0.17	+0.21	1.16	+0.38	0.43
M = Pt; R = Me; A = dtcr (**3a**)	–0.13	+0.40	1.29	+0.53	0.55
M = Pt; R = Et; A = dtcr (**3b**)	–0.17	+0.40	1.33	+0.57	0.58
M = Pd; R = Me; A = mnt (**1a**)	–0.16	+0.46	1.34	+0.62	0.62

[a] The redox potentials are referred to SCE.

In Figure 5 the DC specific conductivity of pressed powder pellets of samples **1a**, **2a**, **2b** and **3a** are shown. These values range from 10^{-11} to $10^{-5}\ \Omega^{-1}\,cm^{-1}$ and increase with increasing temperature according to the Arrhenius law $\sigma = \sigma_0 \exp(-E_a/k_B T)$ (where σ_0 is the pre-exponential factor, E_a is the activation energy, T is the absolute temperature and k_B is Boltzmann's constant). Due to the very large resistance of compound **3a**, only a limited temperature range could be explored. In general the lowest T for each sample corresponds to the lowest current measurable near the picoammeter limit. The pre-exponential factor, σ_0, calculated from the fit, is approximately $0.2\ \Omega^{-1}\,cm^{-1}$ for all compounds and the activation energies range between 0.2–0.6 eV. The value of the conductivity at room temperature, the large value of the activation energy and the fact that σ_0 is constant indicate that these compounds belong to the class of strongly temperature-activated charge-transfer materials, analogous to the segregated stacks systems whose mobility is temperature independent.[17]

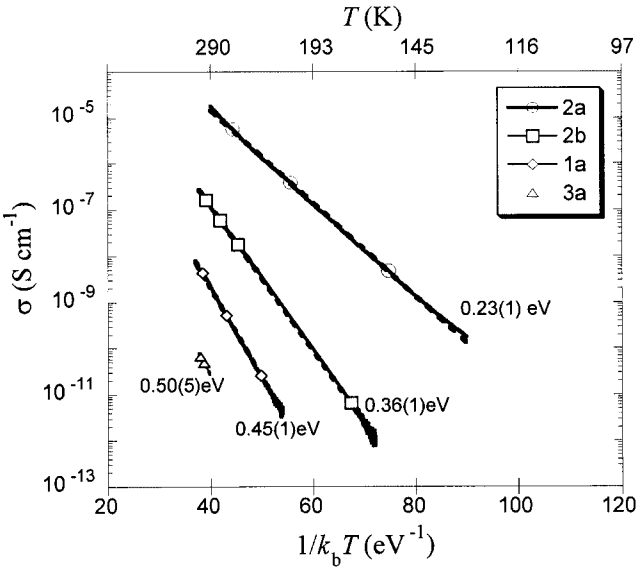

Figure 5. Semilogarithmic plot of the DC conductivity vs. $1/k_bT$, (where k_b = Boltzman costant, T = temperature) for the set of measured compounds. The dotted lines are the best fit of the exponential Arrhenius behaviour. The values of the activation energy E_a are also displayed.

In Figure 6 the σ values at 290 K vs. both the activation energy, E_a, and the free activation enthalpy of electron transfer, ΔG^*, are shown. The data vs. E_a for each compound can be fitted with the equation $\sigma(T_o = 290\ K) = \sigma_0 \exp(-E_a/k_B T_o)$ where σ_0 is approximately $0.2\ \Omega^{-1}\,cm^{-1}$. This behaviour indicates that changes in the conductivity are due only to changes in E_a while the pre-exponential factor σ_0 is approximately the same for all the compounds. For the three Pt salts (**2a**, **2b**, **3a**), where only changes in the nonmetallic sites occur, there is a linear dependence of $\ln\sigma(290K) = a + b\Delta G^*$, with $a \approx 7$ and $b \approx -76$, indicating that for these compounds the transport mechanism within the ion pair is mainly driven by the extent of the charge-transfer interaction, as expected.[18] It is noteworthy that the lnσ(290 K) value for M = Pd (**1a**) does not fall on the same line. Moreover the corresponding lnσ(290 K) vs. ΔG^* dependence for C[ML_2] Kisch salts[18] leads to a linear correlation with different coefficients ($a \approx -3$ and $b \approx -35$). These features suggest that the transport properties and hence the activation energy of CT salts are not simply governed by the activation enthalpy ΔG^*, and some other kind of mechanisms must be involved.

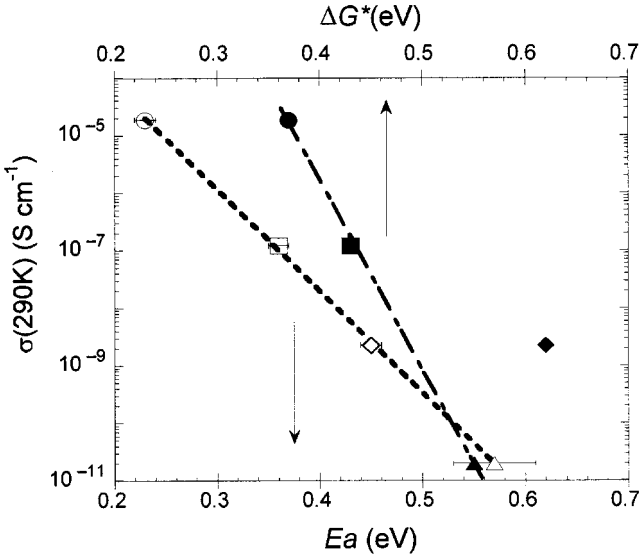

Figure 6. Semilogarithmic plot of the DC conductivity at room temperature vs. the activation energy, E_a, (open symbols) and the free activation enthalpy, ΔG^*, (shaded symbols). The symbols are the same as in Figure 5 (● **2a**, ■ **2b**, ♦ **1a**, ▲ **3a**).

Preliminary photoconductivity measurements have been performed on the two relatively more conducting samples, **2a** and **2b**, by using a lock-in phase, pulsed technique and a halogen lamp (250 W). A low gain in current was observed during illumination. The signal has a decay constant τ of the order of tens of milliseconds and is likely to be related to both the variation of resistance during two different choppered light pulses and to trapping of carriers. The observed photocurrent values I_{ph} ($I_{ph}/I_D \approx 10^{-3}$, where I_D is the dark current) are similar to those reported in Kisch CT salts.[19]

Conclusions

This study has confirmed that cationic and anionic metal-dithiolenes (Pd-Pt) are capable of forming salts that show charge-transfer interactions, responsible for strong NIR CT bands, semiconducting behaviour and photoconducting properties. The properties of these salts are comparable with those of salts formed by dianionic dithiolene metallates with planar organic dications. These properties strongly depend on the amount of electron donation from the donor to the acceptor, which in turn depends on the redox potential and on the planarity of the ionic components of the salt. Since d^8 metal dithiolenes have a rich redox chemistry, which depends on the nature of the substitu-

ents at the C_2S_2 moieties, and determines the nature of their most accessible status while the metal atom imposes the square planar geometry, they offer a wide range of suitable candidates for forming CT salts.

This study also reports the characterisation of $[Pt(R_2pipdt)_2][Pt(dtcr)_2]$, a new example of ion-pair charge-transfer salts formed by an infinite, mixed, planar anion–cation stack. The presence of peripheral C=O groups in the anion produces a net of weak interactions between the N and O atoms of the cation and of the anion inside the stacks thereby favouring the generation of a layer between them. However, these interactions do not overcome the less favourable redox properties of the components with respect to the corresponding mnt salts, that is, promoting anion–cation CT interactions and related properties.

Experimental Section

General Remarks: Reagents and solvents of reagent grade quality were used as supplied by Aldrich. The ligands and the complexes $[Pt(Me_2pipdt)_2](BF_4)_2]$ and $(Bu_4N)_2[Pt(dtcr)_2]$ were prepared according to references [7] and [9]. Microanalyses were performed on a Carlo–Erba CHNS elemental analyser model EA1108. IR spectra (4000–300 cm^{-1}) were recorded on a Bruker IFS55 FT-IR Spectrometer as KBr pellets. Raman spectra (2200–300 cm^{-1}) on single crystal was carried out at room temperature using a Raman microscope (BX, 40, Olympus) spectrometer (ISA xy 800) equipped with a He-Ne (λ = 632,817, Melles-Criot) laser. A 180° reflective geometry was adopted. The sample was mounted on a glass microscope slide and the scattering peaks were calibrated against an Si standard ($\tilde{\nu}$ = 520 cm^{-1}). The spectrum was collected with a 500 s time constant at a 1 cm^{-1} resolution and was averaged over 5 scans. No sample decomposition was observed during the experiments. Electronic spectra (2000–200 nm) were recorded on a Cary 5 spectrophotometer, equipped with a diffuse reflectance accessory. Diffuse reflectance spectra were run on KBr pellets. For electrical measurements the powder samples were pressed up to 0.4 GPa in rectangular bars of (2 × 1 × 13) mm^3 dimensions. Gold electrodes were sputtered on two point-like regions on the surface of the sample in order to favour the ohmic electrical contacts. The DC current measurements were performed by using a Keithley 485 picoammeter and by applying voltages in the range 0–100 V. The temperature was varied by a closed cycle refrigerator system in the range 100–310 K, regulated at the rate of 1 K/min and measured within an error of 1 K.

$[Pt(Me_2pipdt)_2][Pt(dtcr)_2]$ (3a): The blue CH_3CN solution (15 mL) of $(Bu_4N)_2[Pt(dtcr)_2]$ (72 mg; 0.07 mmol) was slowly added to the warm brown CH_3CN solution (20 mL) of $[Pt(Me_2pipdt)_2](BF_4)_2$ (50 mg; 0.07 mmol) and a quantitative precipitation of brown needle-shaped crystals occurred (yield 72 mg; 95%). Crystals suitable for X-ray characterization were grown using a diffusion cell with three compartments connected through porous glass frits. The solutions of the components were introduced in the terminal compartments, and the crystals were collected in the central compartment filled with CH_3CN. $C_{22}H_{20}N_4O_6Pt_2S_8$ (1083.11): calcd. C 24.40, H 1.86, N 5.17, S 23.68; found: C 24.76, H 1.68, N 5.20, S 22.81. IR (KBr pellets): $\tilde{\nu}$ = 3026 vw, 3000 vw, 2920 vw, 2857 vw, 2123 vw, 1684 vs, 1663 vs, 1629 vs, 1618 vs, 1541 s, 1406 ms, 1387 vs, 1362 sh, 1284 mv, 1265 ms, 1238 sh, 1189 m, 1146 mw, 1097 mw, 1064 w, 1027 mw, 924 w, 902 mw, 804 vw, 781 vw, 668 vw, 598 vw, 545 mw, 480 mw, 428 w cm^{-1}. UV/Vis-NIR (reflectance, KBr pellets) λ = 387, 540, 680, 960 nm.

$[Pt(Et_2pipdt)_2][Pt(dtcr)_2]$ (3b): This compound was prepared as described for **3a** (yield 111 mg; 97%), starting from the CH_3CN solutions of $[Pt(Et_2pipdt)_2](BF_4)_2$ (violet; 77 mg; 0.10 mmol) and $(Bu_4N)_2[Pt(dtcr)_2]$ (blue; 102 mg; 0.10 mmol). $C_{26}H_{28}N_4O_6Pt_2S_8$ (1139.22): calcd. C 27.41, H 2.48, N 4.92, S 22.51; found: C 26.73, H 2.52, N 4.86, S 22.65. IR (KBr pellets): $\tilde{\nu}$ = 2980 vw, 2940 vw, 2385 vw, 2350 vw, 2100 w, 1760 w, 1670 vs, 1657 vs, 1638 vs, 1615 sh, 1529 s, 1452 m, 1393 vs, 1360 vs, 1340 sh, 1278 ms, 1261 ms, 1229 ms, 1199 ms, 1126 ms, 1090 w, 1080 w, 1036 w, 970 m, 940 vw, 918 w, 896 m, 858 w, 801 w, 780 w, 760 w, 625 w, 610 w, 550 mw, 476 ms, 421 m, 355 w, 340 mw, 310 vw, 300 vw cm^{-1}. Raman (on single crystal): 2180 vw, 1702 vs, 1412 m, 1192 vs, 1052 vw, 562 vw, 478 s, 422 w cm^{-1}. UV/Vis-NIR (reflectance, KBr pellets) λ = 390, 544, 730, 930 nm.

Acknowledgments

This work was conducted in the framework of the European COST action D14 "Towards New Molecular Inorganic Conductors". The authors thank Prof. Carlo Muntoni, Dipartimento di Fisica dell'Università di Cagliari, for his support.

[1] a) E. I. Stiefel (Ed.), *Dithiolene Chemistry, Progress in Inorganic Chemistry*, John Wiley & Sons **2004**, vol. 52 (see in particular chapter 8 by C. Faulmann, P. Cassoux); b) A. T. Coomber, D. Beljonne, R. H. Friend, J. K. Brédas, A. Charlton, N. Robertson, A. E. Underhill, M. Kurmoo, P. Day, *Nature* **1996**, *380*, 144; c) N. Robertson, L. Cronin, *Coord. Chem. Rev.* **2002**, *227*, 93–127.

[2] a) I. Nunn, B. Eisen, R. Benedix, H. Kisch, *Inorg. Chem.* **1994**, *33*, 5079–5085; H. Kisch, *Coord. Chem. Rev.* **1997**, *159*, 385–396; H. Kisch, B. Eisen, R. Dinnebier, K. Shankland, W. I. F. David, F. Knoch, *Chem. Eur. J.* **2001**, *7*, 738–748.

[3] a) N. S. Hush, *Progr. Inorg. Chem.* **1967**, *8*, 391–444; b) R. A. Marcus, N. Sutin, *Comments Inorg. Chem.* **1986**, *5*, 119–133.

[4] M. Yamashita, A. Ichikawa, T. Hama, T. Ohishi, T. Manabe, H. Miyamae, D. Yoshida, S. Sugiura, H. Kitagawa, Y. Iwasa, T. Mitani, *Mol. Cryst. Liq. Cryst.* **1996**, *284*, 391–398.

[5] a) Z. S. Herman, R. F. Kirchner, G. H. Loew, U. T. Mueller-Westerhoff, A. Nazal, M. C. Zerner, *Inorg. Chem.* **1982**, *21*, 46–56; b) J. Weber, C. Daul, A. Van Zelewsky, A. Goursot, E. Penigault, *Chem. Phys. Lett.* **1982**, *88*, 78–83; c) C. Lauterbach, J. Fabian, *Eur. J. Inorg. Chem.* **1999**, 1995–2004.

[6] S. Curreli, P. Deplano, C. Faulmann, A. Ienco, C. Mealli, M. L. Mercuri, L. Pilia, G. Pintus, A. Serpe, E. F. Trogu, *Inorg. Chem.* **2004**, *43*, 5069–5079.

[7] F. Bigoli, P. Deplano, M. L. Mercuri, M. A. Pellinghelli, L. Pilia, G. Pintus, A.Serpe, E. F. Trogu, *Inorg. Chem.* **2002**, *41*, 5241–5248.

[8] For M = Ni, $[Ni(R_2pipdt)(mnt)]$ mixed-ligand derivatives, which are potential second order non-linear chromophores showing strong negative solvatochromism and β, have been obtained: F. Bigoli, C.-T. Chen, P. Deplano, M. L. Mercuri, M. A. Pellinghelli, L. Pilia, G. Pintus, E. F. Trogu, *Chem. Commun.* **2001**, 2246–2247.

[9] W. B. Heuer, W. H. Pearson, *J. Chem. Soc., Dalton Trans.* **1996**, 3507–3513.

[10] Single crystal X-ray structure determination of **3a**: The data were collected at T = 293 K on an *Enraf–Nonius CAD4* diffractometer (Cu-$K\alpha$; λ = 1.54184 Å). The structures were solved by direct methods (SIR97, **3a**)[20] and refined with full-matrix least-squares (SHELXL-97),[21] using the Wingx soft-

ware package.[22] Crystal data of **3a**: violet needle, $0.25 \times 0.12 \times 0.10$ mm, $C_{22}H_{20}N_4O_6Pt_2S_8$, M_r = 1083.08, triclinic, space group $P\bar{1}$, a = 8.683(2) Å, b = 14.009(5) Å, c = 6.815(2) Å, α = 100.58(4)° β = 92.98(2)°, γ = 106.69(2)°, V = 761.1(4) Å^3, Z = 1, μ = 22.477 mm^{-1}, $\rho_{calcd.}$ = 2.363 g cm^{-3}, $R1$ (w$R2$) = 0.0493 (0.1361) {2747 observed [$I > 2\sigma(I)$] for 2316 independent reflections with 197 parameters}. CCDC-253138 contains the supplementary crystallographic data for this paper. These data can be obtained free of charge from The Cambridge Crystallographic Data Centre via www.ccdc.cam.ac.uk/data_request/cif.

[11] W. B. Heuer, W. H. Pearson, *Polyhedron* **1996**, *15*, 2199–2210.

[12] C. Mealli, D. Proserpio, *J. Chem. Educ.* **1990**, *67*, 399–402.

[13] F. Bigoli, P. Deplano, M. L. Mercuri, M. A. Pellinghelli, G. Pintus, A. Serpe, E. F. Trogu, *J. Am. Chem. Soc.* **2001**, *123*, 1788–1789.

[14] a) C. W. Schläpfer, K. Nakamoto, *Inorg. Chem.* **1975**, *14*, 1338; b) J. L. Wootton, J. I. Zink, *J. Phys. Chem.* **1995**, *99*, 7251–7257; c) S. Kutsumizu, N. Kojima, T. Ban, I. Tsujikawa, *Bull. Chem. Soc., Jpn.* **1987**, *60*, 2547–2553.

[15] K. I. Pokhodnya, C. Faulmann, I. Malfant, R. Andreu-Solano, P. Cassoux, A. Mlayah, D. Smirnov, J. Leotin, *Synth. Met.* **1999**, *103*, 2016–2019.

[16] The contributions of the p_z AO are as follows: oxygen (3%), carbon (6%), sulfur (6%) atoms for each ligand and platinum (d_{xz}, 34%) to the HOMO.

[17] J. Simons, J.-J. André, *Molecular Semiconductors* (Eds.: J. M. Lehn, C. W. Rees), Springer-Verlag, Berlin-Heidelberg, **1985**, chapter 6.

[18] H. Kisch, *Comments Inorg. Chem.* **1994**, 113–132.

[19] H. Meier, H. Kish, *J. Phys. Chem.* **1989**, *93*, 7726–7729.

[20] A. Altomare, M. C. Burla, M. Camalli, G. L. Cascarano, C. Giacovazzo, A. Guagliardi, A. G. G. Moliterni, G. Polidori, R. Spagna, *J. Appl. Crystallogr.* **1999**, *32*, 115–119.

[21] G. M. Sheldrick, *SHELX97*. Programs for Crystal Structure Analysis (**1997**) (Release 97-2), University of Göttingen, Germany.

[22] L. J. Farrugia, *J. Appl. Crystallogr.* **1999**, *32*, 837–838.

Received: October 20, 2004
Published Online: April 11, 2005

